Modeling and experimental study on dielectric elastomers incorporating humidity effect

Junshi Zhang[1], Xuejing Liu[2], Lei Liu[3], Zhichun Yang[1(a)], Pengfei Li[3] and Hualing Chen[4]

[1] *School of Aeronautics, Northwestern Polytechnical University - Xi'an 710072, China*
[2] *School of Mechanical and Electrical Engineering, Xi'an Polytechnic University - Xi'an 710048, China*
[3] *School of Mechanical and Precision Instrument Engineering, Xi'an University of Technology - Xi'an 710048, China*
[4] *State Key Laboratory of Strength and Vibration of Mechanical Structures, Xi'an Jiaotong University*
Xi'an 710049, China

Abstract – In this research, we carry out a modeling and experimental study on the performance of a VHB 4910 elastomer considering the humidity effect. Firstly, based on the uniaxial tension test of VHB 4910, it is concluded that humidity leads to a reduction of the shear modulus. Subsequently, the static electromechanical performance of VHB 4910 is explored, which implies that voltage-induced deformation increases gradually with the increasing humidity. Finally, by applying a sinusoidal voltage, the humidity effect on the resonance properties of the VHB 4910 elastomer is found to decrease the resonant frequency and augment the vibration intensity.

As the electro-active polymers, dielectric elastomers (DEs) can be induced to generate a fast and large deformation when a high voltage is applied across the thickness direction [1–6]. Under a combination actuation of high voltage and air pressure, the maximum areal deformation can be larger than 2200% [7], demonstrating significant potential applications as soft actuators, energy harvesters, and biomimetic transducers [8–12].

The majority of DE materials belong to macromolecular polymers, which are greatly affected by the external environmental factors, including temperature [13–16] and humidity [17–19]. Among various DE materials, VHB 4910 (a polyacrylic film) has been extensively investigated in recent years, due to its unique large deformability. The researchers have found that the temperature effect plays an important role in determining the electromechanical actuation of DEs [13–16]. However, the humidity effect on DEs still lacks the necessary attention. In 2013, Biggs *et al.* [17] found that the increasing humidity decreases the mean cycles to failure of acrylic DEs when subject to an AC voltage. Then Chen *et al.* [18] experimentally investigated the effect of humidity on the electrical breakdowns of the VHB 4905 film. Subsequently, by using the silicone

DE film, Fasolt *et al.* [19] studied the breakdown field with consideration of the humidity effect. In our recent study [20], the dielectric constant and voltage-induced deformation of VHB 4910 film under different ambient humidity levels were experimentally investigated.

In this study, following our previous research [20], we further explore the humidity effect on the actuation properties of VHB 4910 both theoretically and experimentally. Firstly, by employing the uniaxial tension, the stress-stretch curve of the VHB 4910 film is measured under different humidity levels, where the temperature is set to room temperature (20 °C). The VHB 4910 samples and mechanical testing setups are shown in fig. 1.

In the test, the VHB 4910 piece is firstly cut into a strip shape (4 mm × 30 mm) and fixed between two clamped frames. Then the stress-strain curve of VHB 4910 is measured with a micro-force tensile testing machine (ZQ-60B, Zhiqu™) in an airtight container. The prescribed humidity can be approximately tuned by different saturated salt solutions [20–22], including potassium acetate (CH_3COOK), potassium carbonate (K_2CO_3), sodium bromide (NaBr) and potassium bromide (KBr), which are placed in the airtight container. The VHB 4910 samples are uniaxially stretched to a maximum strain of 400% under different humidity levels. The stress-strain curve of

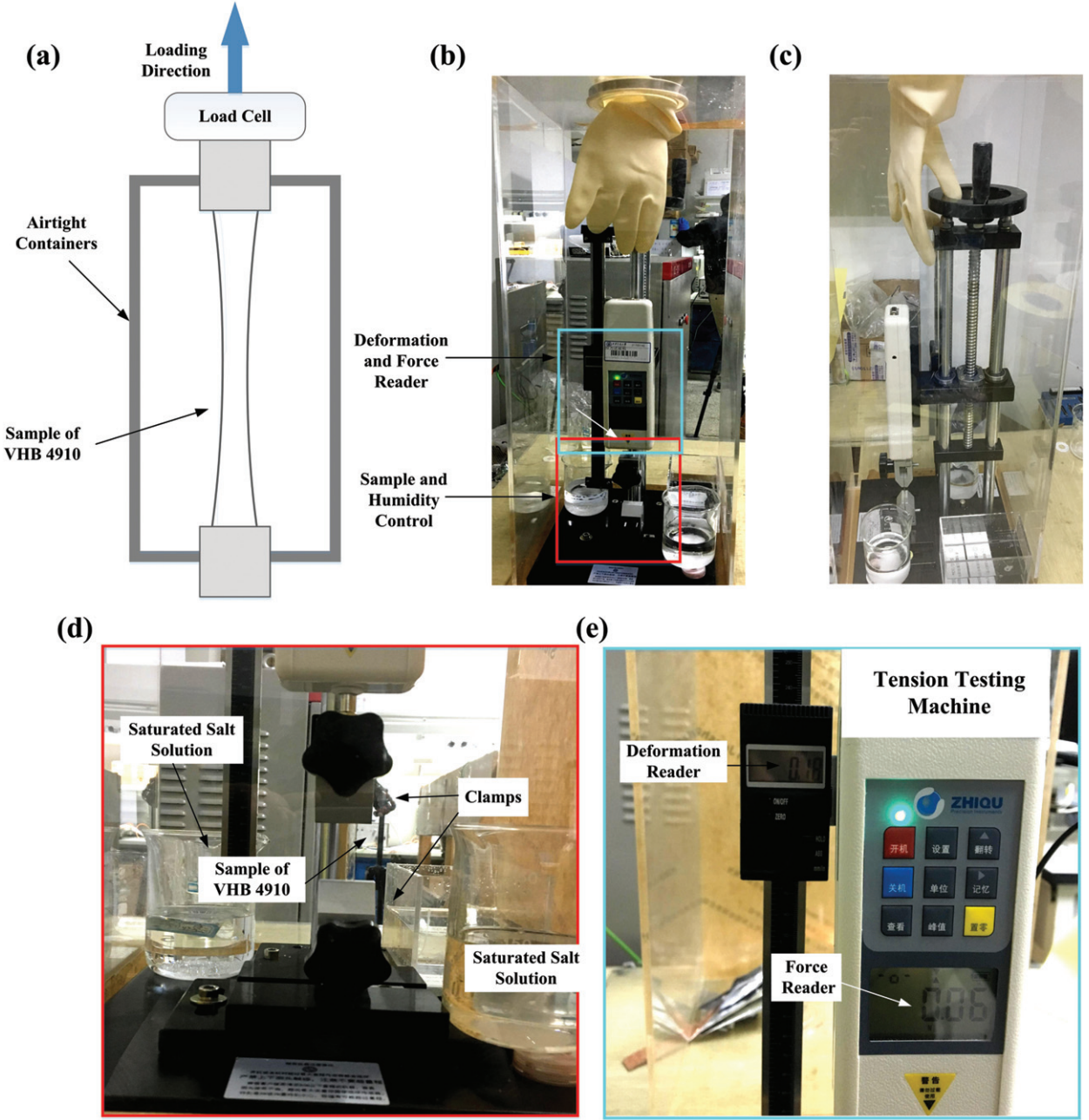(a)E-mail: yangzc@nwpu.edu.cn (corresponding author)

Fig. 1: Mechanical testing setup of uniaxial tension of the VHB 4910 film under different humidity levels.

the VHB 4910 piece is obtained through data processing, which is shown by the symbols in fig. 2(a). In order to eliminate the errors, 3 samples are carried out for each measurement, and an average value is adopted as experimental results. The solid lines in fig. 2(a) represent the nonlinear fitting results, which are detailed as follows. The Gent model [23] is usually utilized to characterize the strain energy density of the VHB elastomer, that is,

$$W = -\frac{J_{\lim}}{2}\mu\left(H\right)\log\left(1 - \frac{\lambda_1^2 + \lambda_2^2 + \lambda_3^2 - 3}{J_{\lim}}\right), \quad (1)$$

where $\mu(H)$ is the humidity-dependent shear modulus of VHB 4910, λ_1, λ_2, and λ_3 are the stretches in the three

principal directions, $J_{\lim}$ is the material constant related to the limiting stretch. Due to the incompressible assumption [3], we have $\lambda_1\lambda_2\lambda_3 = 1$. Thus, with reference to thermodynamics, the stress of the uniaxial-tensioned DE is calculated as

$$\sigma_{UT} = \mu(H)\frac{\lambda_{UT}^2 - \lambda_{UT}^{-1}}{1 - (\lambda_{UT}^2 + 2\lambda_{UT}^{-1} - 3)/J_{\lim}}, \quad (2)$$

where σ_{UT} and λ_{UT} denote the stress and stretch of VHB 4910 in uniaxial tension, respectively. As can be seen in fig. 2(a), the solid lines are obtained by fitting the experimental data with eq. (2), and the fitting results are given
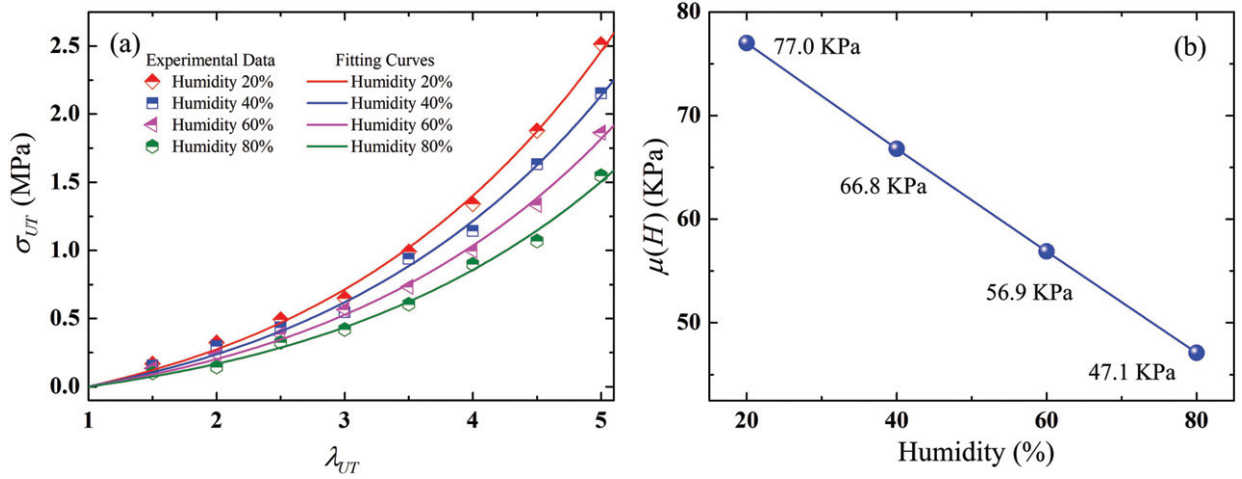
Fig. 2: Uniaxial tension of the VHB 4910 film. (a) Comparison between the experimental data and the theoretical fitting of the VHB 4910 film under different humidity levels (20%, 40%, 60%, and 80%). (b) Shear modulus of the VHB 4910 film under different humidity levels (20%, 40%, 60%, and 80%).
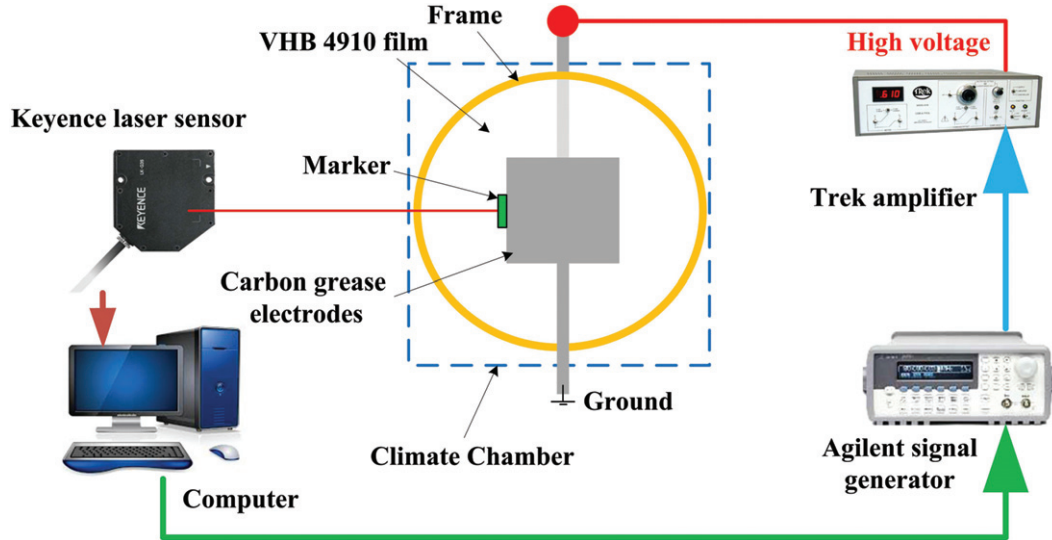

Fig. 3: Electromechanical testing setups and procedures of the VHB 4910 film under different humidity levels.

in fig. 2(b). From both experimental and theoretical results, it is noted that for a prescribed stretch ratio, the humidity reduces the stress of VHB 4910, which implies that the VHB 4910 film becomes softer with the increasing humidity. Furthermore, such a conclusion can be proved by fig. 2(b), in which it is obvious that the shear modulus reduces approximately linearly. That is, when the humidity increases from 20% to 80%, the shear modulus of VHB 4910 reduces from $77.0 \, \text{KPa}$ to $47.1 \, \text{KPa}$.

Based on the above analyses on the mechanical performances, in the following, we investigate the humidity effect on the static electromechanical properties of VHB 4910 films. The electromechanical testing setups and procedures are illustrated in fig. 3. The temperature is also set to room temperature, $i.e.$, $20\,°\text{C}$. The VHB 4910 film is equal-biaxially prestretched and clamped by a pair of annular frames. In the experimental measurement, 3 groups

of prestretch ratios (2×2, 3×3, 4×4) are tested. The carbon grease electrodes (No. 846, MG Chemicals) are coated in the center area of both surfaces, forming a square configuration with a length of $L = 20 \, \text{mm}$. A voltage amplifier (Model 610E, Trek) is utilized to produce the high voltage for actuation, and a signal generator (6811B, Agilent) is used to generate the required voltage signal. A laser sensor (LK-G150/G10, Kenyence) is employed to measure the electromechanical displacement of the VHB 4910 film, by attaching a lightweight marker on the edge of the electroactive area. The various humidity levels are controlled and tuned by a Climate Chamber (MHL-02S/12, Yoma) [20].

Theoretical modeling is simultaneously performed for the explorations of the electromechanical properties of the VHB elastomer. By employing thermodynamics and the Gent model, and assuming a homogeneous deformation, the constitutive relation of the DE actuator is expressed as
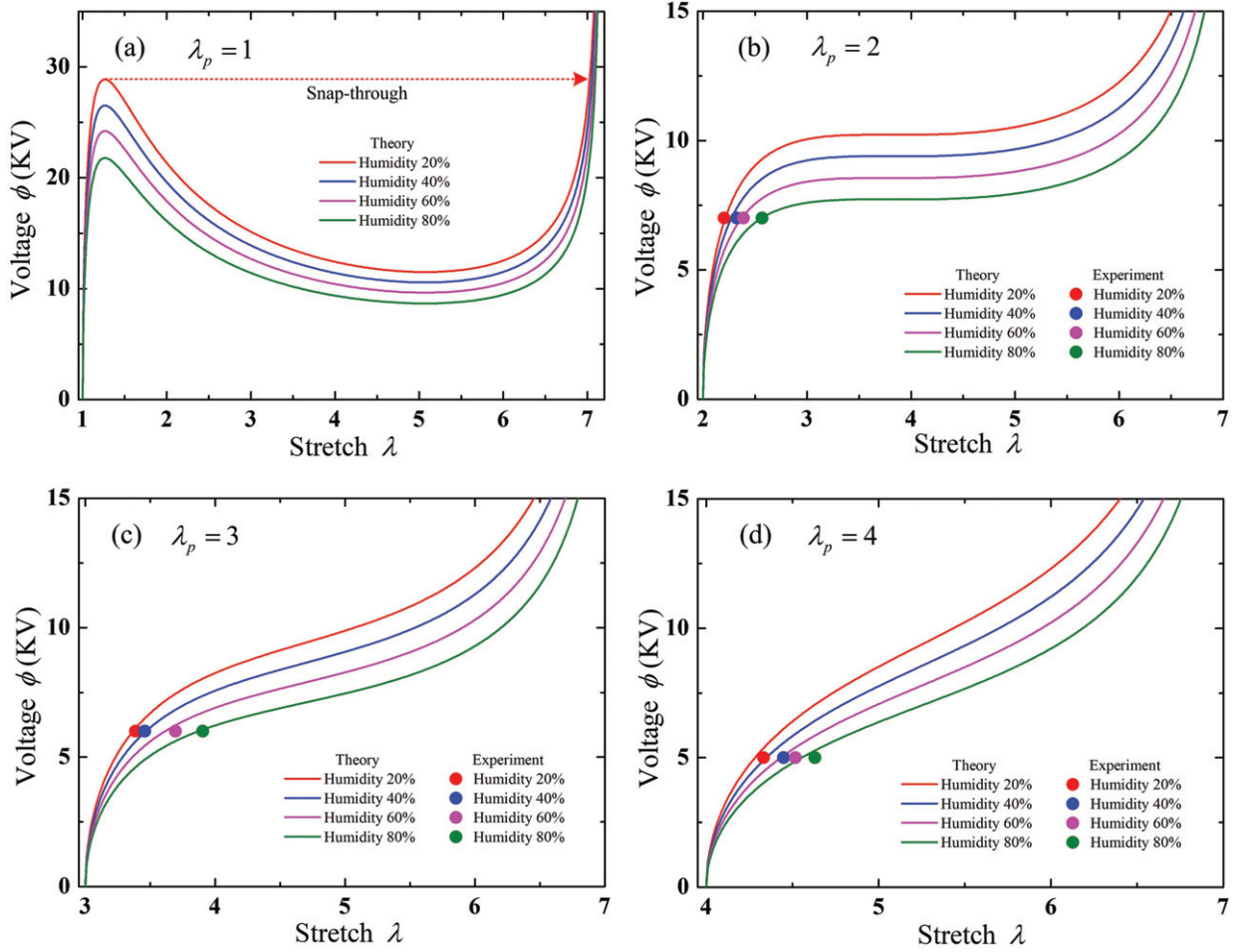
Fig. 4: Comparison of static electromechanical deformation between theoretical modeling and experimental data of VHB 4910 films under different humidity levels (20%, 40%, 60%, and 80%) and prestretch ratios. (a) $\lambda_p = 1$, (b) $\lambda_p = 2$, (c) $\lambda_p = 3$, (d) $\lambda_p = 4$.

$$\frac{\sigma_p}{\lambda_p}\lambda + \varepsilon\left(H\right)\left(\frac{\phi}{L_3}\right)^2\lambda^4 = \frac{\mu\left(H\right)\left(\lambda^2 - \lambda^{-4}\right)}{1 - \left(2\lambda^2 + \lambda^{-4} - 3\right)/J_{\lim}}, \quad (3)$$

where λ is the in-plane stretch; $\varepsilon(H)$ is the humidity-dependent dielectric constant; ϕ is the applied voltage; $L_3 = 0.001\,\mathrm{m}$ is the original thickness of the VHB 4910 film; λ_p is the prestretch; σ_p is the prestress that is acquired to attain the prestretch λ_p, and is regarded as a constant in the theoretical modeling [20,24], that is,

$$\sigma_p = \frac{\mu\left(H\right)\left(\lambda_p^2 - \lambda_p^{-4}\right)}{1 - \left(2\lambda_p^2 + \lambda_p^{-4} - 3\right)/J_{\lim}}. \quad (4)$$

As reflected in eq. (3), the dielectric constant should be known for the theoretical simulation. Based on our previous research [20], the dielectric constant of VHB 4910 under different humidity levels and prestretch ratios are given in table 1. It is noted that for a prescribed prestretch ratio, the dielectric elastomer increases gradually with the increasing humidity.

Accordingly, the static electromechanical deformation of the VHB 4910 elastomer under different humidity levels

Table 1: Dielectric constant of VHB 4910 films under different humidity levels and prestretch ratios.

Humidity	$\lambda_p = 1$	$\lambda_p = 2$	$\lambda_p = 3$	$\lambda_p = 4$
20%	4.96	4.63	4.21	3.65
40%	5.10	4.76	4.34	3.81
60%	5.21	4.89	4.44	3.91
80%	5.33	4.96	4.52	3.96

is shown in fig. 4. When the prestretch ratio is $\lambda_p = 1$ (fig. 4(a)), it is difficult to obtain the experimental data, therefore, we only give theoretical predictions. It can be seen that, when $\lambda_p = 1$, VHB 4910 experiences snap-through instability [25,26], despite the humidity. When the prestretch ratio increases to $\lambda_p = 2$, snap-through instability barely disappears, resulting from the tension induced by the prestretch, as illustrated in fig. 4(b). On the other hand, it is more clearly seen that humidity leads

to an enlargement of the voltage-induced deformation. In addition, it can be seen that the experimental data agree well with the theoretical result, demonstrating the reliability of the established model. Furthermore, when the prestretch ratio enlarges to $\lambda_p = 3$ and $\lambda_p = 4$, similar conclusions can be drawn, that is, the static electromechanical deformation of VHB 4910 increases gradually when the humidity increases, which is presented in figs. 4(c) and (d). However, it seems that there is an increase in the differences between the experimental data and the theoretical predictions with the increasing prestretch ratio. Such increasing difference can be attributed to the measuring errors and the simplification of theoretical modeling.

Finally, the effect of humidity on the nonlinear dynamic properties of the VHB 4910 elastomer is investigated, where the inertial force should be considered. For the square DE actuator sketched in fig. 3, the work done by the inertial force can be calculated along the length direction [27,28]. Hence, the dynamic governing equations can be expressed as

$$\frac{\rho L^2}{3}\frac{\mathrm{d}\lambda^2}{\mathrm{d}t^2} + \frac{\mu(H)(\lambda - \lambda^{-5})}{1 - (2\lambda^2 + \lambda^{-4} - 3)/J_{\lim}}$$
$$- \frac{\sigma_p}{\lambda_p} - \varepsilon(H)\left(\frac{\phi}{L_3}\right)^2 \lambda^3 = 0, \qquad (5)$$

where $\rho = 1.2 \times 10^3\,\mathrm{kg/m^3}$ [29] is the density of VHB 4910; $L = 20\,\mathrm{mm}$ is the length of the active area of the square DE actuator. In order to obtain the dynamic vibration, the sinusoidal voltage is applied, that is, $\phi = \phi_0 \sin(2\pi f t)$, where ϕ_0 and f are the amplitude and frequency of the applied voltage, respectively. Therefore, the effect of humidity on the resonant properties of the VHB 4910 piece is explored. We define the half-value of the maximum difference between the peak and valley value of λ as λ_{P-V} [30,31], which is utilized to describe the vibration intensity. In the whole frequency range, it is assumed that the resonance occurs when λ_{P-V} peaks, and the corresponding frequency is regarded as the resonant frequency. Under the condition of $\phi_0 = 3000\,\mathrm{V}$ and $\lambda_p = 2$, the frequency response spectrum of the VHB 4910 elastomer under different humidity levels is revealed in fig. 5.

An obvious finding is that the humidity effect leads to a reduction of the resonance frequency. When the humidity level is 20%, the resonant frequency is obtained as 63.057 Hz, however, the resonant frequency decreases to 48.726 Hz when the humidity is 80%. On the other hand, it is noted that the increase of humidity can induce an increase of λ_{P-V}, implying that the humidity can amplify the vibration intensity, which is similar to the static properties shown in fig. 4. Another effect of the frequency response spectrum is the harmonic resonance [31], that is, the superharmonic resonance occurs when the frequency is about half the resonance frequency, and the subharmonic resonance occurs when the frequency is about twice the resonance frequency.
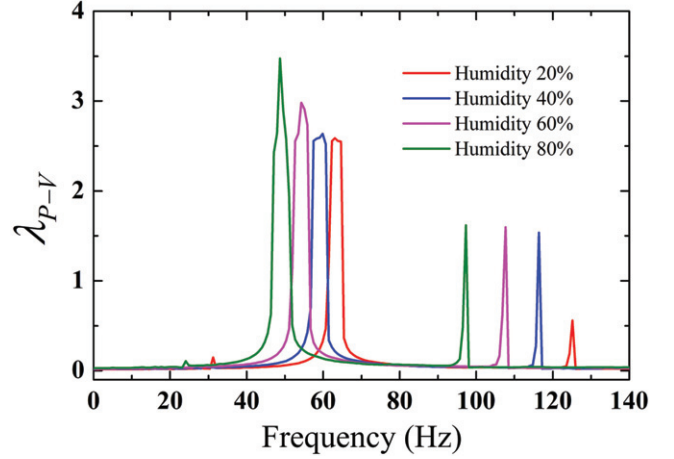

Fig. 5: The frequency response spectrum of the VHB 4910 elastomer under different humidity levels.

In this paper, we develop a modeling and experimental study on the electromechanical performance of a VHB elastomer, considering the humidity effect. The uniaxial tension test is performed to obtain the shear modulus of the VHB 4910 elastomer under different humidity levels. It is found that the humidity effect induces a reduction of the shear modulus of the VHB 4910 elastomer. Based on this, an electromechanical-constitutive model of the VHB elastomer is established incorporating the humidity effect, where the electromechanical measurements are simultaneously carried out. The experimental data show good agreement with theoretical predictions, demonstrating that the electromechanical deformation increases gradually with the increasing humidity. Finally, the effect of humidity on the resonant properties of the VHB 4910 piece is investigated, and the results show that the humidity causes a reduction of the resonant frequency and an increase of the resonance intensity. This research can be utilized to optimize the DE actuators working in some extremely humid environmental conditions, so as to advance the development of DE-based soft robots.

$$* * *$$

REFERENCES

[1] Pelrine R., Kornbluh R., Pei Q. and Joseph J., *Science*, **287** (2000) 836.
[2] Zhu J. and Luo J., *EPL*, **119** (2017) 26003.
[3] Suo Z., *Acta Mech. Solida Sin.*, **23** (2010) 549.
[4] Zurlo G., Destrade M., DeTommasi D. and Puglisi G., *Phys. Rev. Lett.*, **118** (2017) 078001.

[5] XIAO R., *EPL*, **114** (2016) 16002.

[6] ZHANG J., *EPL*, **128** (2019) 37003.

[7] AN L., WANG F., CHENG S., LU T. and WANG T. J., *Smart Mater. Struct.*, **24** (2015) 035006.

[8] LIU Y., LIU L., ZHANG Z., JIAO Y., SUN S. and LENG J., *EPL*, **90** (2010) 36004.

[9] LI T. *et al.*, *Sci. Adv.*, **3** (2017) e1602045.

[10] ZHAO J., WANG S., XING Z., MCCOUL D., NIU J., HUANG B., LIU L. and LENG J., *Smart Mater. Struct.*, **25** (2016) 075025.

[11] ZHOU J., JIANG L. and KHAYAT R., *EPL*, **115** (2016) 27003.

[12] WANG W. and AHN S.-H., *Soft Robot.*, **4** (2017) 379.

[13] ZHAO H., ZHANG L., YANG M.-H., DANG Z.-M. and BAI J., *Appl. Phys. Lett.*, **106** (2015) 092904.

[14] LIU L., LIU Y., YU K. and LENG J., *Mech. Mater.*, **72** (2014) 33.

[15] LAI S. K., BATRA A. and COHEN C., *Polymer*, **46** (2005) 4204.

[16] LIU L., CHEN H., LI B., WANG Y. and LI D., *Appl. Phys. Lett.*, **107** (2015) 062906.

[17] BIGGS J. *et al.*, *Angew. Chem., Int. Ed.*, **52** (2013) 9409.

[18] CHEN B., KOLLOSCHE M., STEWART M., BUSFIELD J. and CARPI F., *Proc. SPIE*, **9798** (2016) 97980Q.

[19] FASOLT B., WELSCH F., JANK M. and SEELECKE S., *Smart Mater. Struct.*, **28** (2019) 094002.

[20] LIU X., ZHANG J. and CHEN H., *Appl. Phys. Lett.*, **115** (2019) 184101.

[21] CAROTENUTO A. and DELL'ISOLA M., *Int. J. Thermophys.*, **17** (1996) 1423.

[22] O'BRIEN F. E. M., *J. Sci. Instrum.*, **25** (1948) 73.

[23] GENT A. N., *Rubber Chem. Technol.*, **69** (1996) 59.

[24] BAI Y., JIANG Y., CHEN B., FOO C. C., ZHOU Y., XIANG F., ZHOU J., WANG H. and SUO Z., *Appl. Phys. Lett.*, **104** (2014) 062902.

[25] ZHAO X. and SUO Z., *Phys. Rev. Lett.*, **104** (2010) 178302.

[26] AN S.-Q., ZOU H.-L. and DENG Z.-C., *J. Phys. D: Appl. Phys.*, **52** (2019) 195301.

[27] ZHANG J., CHEN H., LI B., MCCOUL D. and PEI Q., *Soft Matter*, **11** (2015) 7483.

[28] LI T. QU S. and YANG W., *Int. J. Solids Struct.*, **49** (2012) 3754.

[29] XU B.-X., MUELLER R., THEIS A., KLASSEN M. and GROSS D., *Appl. Phys. Lett.*, **100** (2012) 112903.

[30] ZHANG J., CHEN H. and LI D., *Phys. Rev. Appl.*, **8** (2017) 064016.

[31] ZHU J., CAI S. and SUO Z., *Polym. Int.*, **59** (2010) 378.